ICSV14
Cairns • Australia
9-12 July, 2007

OCEAN ACOUSTIC INTERFEROMETRY EXPERIMENT

Laura A Brooks[1 2*], Peter Gerstoft[1]

[1]Marine Physical Laboratory, Scripps Institution of Oceanography, La Jolla, CA

[2]School of Mechanical Engineering, the University of Adelaide, SA 5005, Australia

[*]laura.brooks@mecheng.adelaide.edu.au

Abstract

Ocean acoustic interferometry (OAI) is a technique which relates the cross-correlations from a line of active sources to two receivers within a waveguide, and the time domain Green's function between said receivers. Within this paper, three specific OAI source geometries are briefly introduced and explained. Experimental OAI data were collected during the SW06 (Shallow Water '06) sea trials during September 2006. Preliminary analysis of the data shows that the cross-correlations exhibit an observable structure.

1. INTRODUCTION

Approximation of the Green's function between two points in both open and closed environments has been a subject of interest over the last few years. Lobkis and Weaver[1] showed, both theoretically and experimentally, that the Green's function between two points can be determined from their temporal cross-correlation within a diffuse ultrasonic field. This concept was extended by Derode *et al.*[2] who showed that the Green's function can be conditionally recovered in an open scattering medium. They concluded that the Green's function will only emerge from cross-correlations within an open scattering medium if the cross-correlations are summed over a perfect time-reversal mirror. Wapenaar[3] and Van Manen *et al.*[4] demonstrated that retrieval of the Green's function through summed cross-correlations can also be achieved in an inhomogeneous medium.

Extraction of the Green's function by cross-correlation from ultrasonic noise[5, 6, 7], ambient noise in a homogeneous medium[8], ambient ocean acoustic noise[9, 10, 11], seismic noise[12, 13, 14, 15], and even moon-seismic noise[16], has been undertaken, and the governing concepts are now quite well understood.

In a separate paper by the authors[17], the relationship between cross-correlations from a vertical line of active sources to two receivers within a waveguide, and the shaded time domain Green's function between said receivers, is discussed. The use of an active source for this purpose was coined ocean acoustic interferometry (OAI), as it is related to classical and seismic interferometry[18], where interferometry refers to the determination of information from the interference phenomena between pairs of signals. It was shown that in an isovelocity waveguide, the stacked cross-correlations show very good agreement with the $|S(\omega)|^2/\omega$ amplitude, and $3\pi/4$ phase, shaded Green's function. Numerical simulations of OAI were used to confirm the theoretical findings and also to show what can happen in a more complex environment. Results agreed with the modal based approach of Roux and Fink[20].

Within this paper, OAI experiments which were conducted during the SW06 (Shallow Water '06) sea trial are described. A graphical display of some of the data collected is presented.

2. BACKGROUND

Consider the waveguide depicted in Fig. 1(a). The x and z directions are defined, respectively, as the horizontal axis and the vertical axis. A vertical line of sources is uniformly and densely distributed within the vertical plane containing receivers A and B, external to the two receivers, and closer to B. The sum of the cross-correlations of the signals

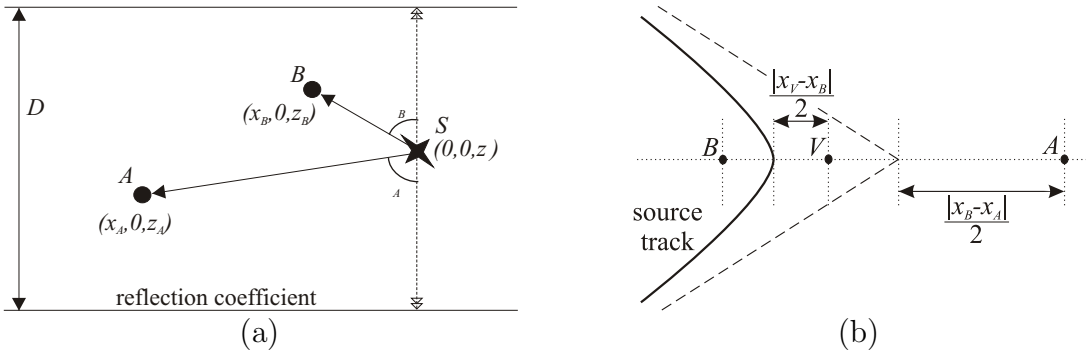

Figure 1. Source-receiver geometry (a): the source S is located at (0,0,z), and receivers A and B are located at (x_A,0,z_A) and (x_B,0,z_B) respectively within a waveguide of depth D. Hyperbolic source track as viewed from above (b): the hyperbola apex passes midway between receiver A and virtual receiver B and the asymptote is midway between B and A.

received at A and B (adapted from Snieder *et al.*[21]) in the frequency domain is

$$C_{AB}(\omega) = |\rho_s S(\omega)|^2 n \int_0^D G(\mathbf{r}_A, \mathbf{r}_S) G^*(\mathbf{r}_B, \mathbf{r}_S)\, dz, \tag{1}$$

where ρ_s is the density at the source, $S(\omega)$ is the source spectrum, n is the number of sources per unit length, $G(\mathbf{r}_\psi, \mathbf{r}_S)$ is the Green's function between the source S, and receiver ψ, and * denotes complex conjugation. The lower bound of the integral is 0 since the waveguide has a free surface at $z = 0$ and the upper bound is the waveguide depth D since there are no reflective surfaces below this depth. Using the method of stationary phase[19], it was shown by the authors that the sum of the cross-correlations can be related to the Green's function between A and B by calculating the cross-correlation for each source depth and then summing (also known as 'stacking') the result:

$$C_{AB}(\omega) = e^{i(3\pi/4)} n |S(\omega)|^2 \sum_{z_s} \left(\frac{\Gamma^{b_A+b_B} \rho_s^2 \, G_f\left(R\left(z_s\right)\right)}{\sin\phi_s} \sqrt{\frac{\left(\frac{1}{L_B(z_s)} - \frac{1}{L_A(z_s)}\right) c}{8\pi\omega}} \right), \tag{2}$$

where Γ is the reflection coefficient of the bottom, b_ψ is the number of bottom bounces for a given path, ϕ is the acute angle between the path and the vertical at the point of departure from the source, $L_\psi = \sqrt{x_\psi^2 + (2b_\psi D \pm z \pm z_\psi)^2}$ is the length of the given path between the source S and receiver ψ, and the summation is over all stationary points, z_s. The term $G_f = e^{ikR}/(4\pi R)$ is the 3D Green's function within a homogeneous medium, where k is the wave number and R is the distance from the source.

OAI can be performed using a horizontal line of sources (i.e., a towed source) instead of a vertical source column. The source is towed along the horizontal line defining the vertical plane containing both receivers, starting directly above one receiver, and travelling away from the receivers. In this case, the summed cross-correlation is related to the Green's function by the relationship:

$$C_{AB}(\omega) = e^{i(3\pi/4)} n |S(\omega)|^2 \sum_{x_s} \left(\frac{\Gamma^{b_A+b_B} \rho_s^2 \, G_f\left(R\left(x_s\right)\right)}{\cos\phi_s} \sqrt{\frac{\left(\frac{1}{L_B(x_s)} - \frac{1}{L_A(x_s)}\right) c}{8\pi\omega}} \right). \quad (3)$$

OAI using a straight line tow source relies on the fact that the horizontal distance from the source to receiver A is always $x_A - x_B$ further than to receiver B. There exists a second tow-source configuration in which the horizontal distance to each receiver differs by a constant amount (see derivation in Appendix A): a hyperbola which has its asymptotic origin at the point midway between A and B, its x-intercept at the midpoint between B and a virtual receiver V (located between the two physical receivers at the same depth as the first receiver), and its focus at B (see Fig. 1(b)). The hyperbolic tow-source can be considered to be a similar geometrical set-up as the straight line scenario, although in this case, the horizontal difference in path length is a constant value of $x_A - x_V$. The resulting cross-correlation sum will therefore relate to the Green's function between the virtual receiver V and receiver A rather than the Green's function between the two physical receivers B and A.

All three OAI scenarios (source column, straight line towed source and hyperbolic towed source) have their advantages and drawbacks. The source column is performed in a region close to both receivers and therefore attenuation is minimal, but suffers from there being no sources in the underlying sediment and hence the modal continuum of the sediment is not fully accounted for[20, 17].

The towed source scenarios are advantageous in that once the source is deployed the only consideration is the ship path; however, they suffer from stationary-phase contributions from correlations between a wave that initially undergoes a surface reflection and one that does not (for an isovelocity water column, one wave departs at an angle of ϕ from the horizontal and the other departs at an angle of $-\phi$)[10, 17]. These stationary-phase contributions are intrinsic to the horizontal source configuration. If the source depth is reduced, the spurious arrivals converge to the same travel time as the true Green's function paths; however, they are π out of phase and will result in shading of the Green's function. The hyperbolic towed source method is the only non 'end-fire' (i.e., source located in the vertical plane defined by the two receivers) tow-source geometry which is feasible. The source must, in this case, have its apex at a location horizontally between two physical hydrophones. It has the advantages of being accessible even when buoys mark the beginning and end of arrays, and also of being able to approximate the Green's function between a physical receiver and a virtual receiver; however, it suffers from the disadvantages that the hyperbola can be difficult for a ship to navigate, and the theory assumes range independence.

3. EXPERIMENT

The SW06 (Shallow Water 2006) experiment was a large scale collaborative shallow water acoustic experiment, combining both low frequency and medium frequency acoustics tests, conducted off the East Coast of the US. The experiments pertinent to this research were conducted during the first week of September 2006 from the deployment vessel *R/V Knorr*. Data was collected for all three of the OAI source configurations previously described:

source column, straight line towed source and hyperbolic towed source.

The data was recorded upon SWAMI 32, an L-shaped array owned by ARL-UT (Applied Research Laboratories, The University of Texas at Austin). The vertical portion of the array (VLA) originally consisted of 12 hydrophones, evenly spaced at 5.95 m intervals, but the lowest two hydrophones had to be tied off prior to deployment due to the water column depth being less than anticipated, resulting in a 10-hydrophone array. The depth of the water column at this location was 68.5 m. The horizontal portion of the array (HLA) consisted of 20 hydrophones which were spaced at increments that continuously decreased as the distance from the VLA was increased. The total length was 256.43 m. The geometrical configuration of the array is depicted in Fig. 2(a).

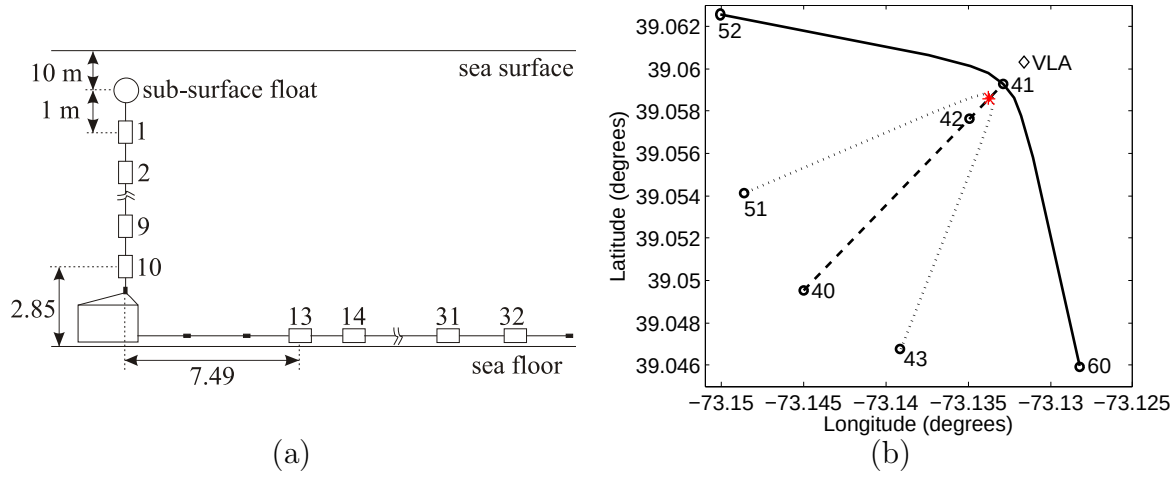

Figure 2. Experimental geometry and track: (a) geometrical configuration of the SWAMI32 L-shaped array, and (b) experimental site where numbered markers are waypoint numbers, 'VLA' is the location of the vertical portion of the SWAMI32 array, and the end of the horizontal portion of the array is marked by an asterix.

Two towed sound sources were used: an ITD mid-frequency source emitting a 1200 − 2900 Hz LFM signal, and a J-15-1 low frequency source emitting a 100 − 900 Hz LFM signal. The experimental track geometry is depicted in Fig. 2(b). The VLA is marked on the figure and the horizontal array extends from this location and terminates at the point marked by a star. The experimental site is in close proximity to well surveyed areas and therefore there exists sufficient data to establish reasonable ground truths. Water column properties were recorded numerous times throughout the experiment using Sea-bird 911*plus* CTD instrumentation.

The mid-frequency experiments were all carried out on September 3 2006. The hydrophone sensitivity was set to −200 dB re 1 V/μPa. A storm had passed through less than twenty four hours earlier and hence, despite the low wind levels, a significant amount of swell remained in the sea. The ITD source was towed at a set-point depth of 10 m, but due to the remnant swell, the source depth varied from this value by up to 1 m. The source level was set to 170 dB.

At WP42 (waypoint 42), located 150 m at end-fire from the end of the HLA, the source was lowered from 10 m to 60 m at a constant rate of 1 m/min. Upon completion of this event the source was returned to the original 10 m depth, and the vessel proceeded to WP40, located at end-fire to the horizontal array at a range of 1400 m from the last array element. The source was towed along the dashed path from WP40 to WP41, located midway between hydrophones 16 and 30, at 1 knot. The ship proceeded to WP43 and then sailed at 1.5 knots along the dotted hyperbolic path (hyperbola-1) to WP51. The ship then proceeded to WP52 and sailed along the solid hyperbolic path (hyperbola-2) to WP60.

The difference between the two hyperbolae is how narrow they are. Hyperbola-1 was designed such that its focal point coincides with hydrophone 30, its apex is at a point midway between hydrophones 30 and 28, and its asymptotic origin is at a point midway between hydrophone 30 and the VLA. Hyperbola-2 has the same focal point and asymptotic origin, but the apex is midway between hydrophones 30 and 16.

The low frequency experiments were performed on September 5 2006. The hydrophone sensitivity was set to -180 dB re 1 V/μPa. The seas were more calm on this day and therefore the J-15-1 source was able to be held within 0.15 m of the 10 m set-point value. The source level was maintained at 160 dB throughout the experiment. The ship sailed along the end-fire track from WP40 to WP41 at 1 knot. Approximately 4.5 hours after the completion of this event a source lowering took place at WP42. The source was lowered from 1 m to 60 m depth at a constant rate of 1.84 m/s.

3.1. Data analysis

Initial analysis of the low frequency data (100-900 Hz) showed that it contains a relatively high proportion of ship and other background noise. Even after ship tonals were bandpass-filtered out, the resultant data had a poor SNR. The mid-frequency data (1200-2900 Hz) had a much better SNR and hence was selected for further analysis. For each experiment the data was bandpass filtered to eliminate low frequency background and ship noise. Cross-correlation between the signals received at hydrophones 5 and 30 as a function of time are shown in Fig. 3 for four sets of mid-frequency data: (a) source lowering, (b) end-fire track, (c) hyperbola-1, and (d) hyperbola-2. For display purposes a correlation of 1 s duration has been performed every 50 s (100 s for hyperbola-1).

For each graph in Fig. 3 the cross-correlations can be seen to evolve with time. Each individual peak in the correlation occurs at a correlation time equal to the difference between the time the signal takes to travel to A by a certain path and the time it takes to travel to B by another path. These peaks will migrate to a higher correlation time as experimental time increases if the path length difference increases and to a lower time if it decreases.

For the source lowering (a), the time at which the correlation was performed was zero when the source was initially at 9.8m, and was approximately 2900 s when the source was at 60 m. As the source was lowered the cross-correlations tended to converge slightly toward the central value of approximately 0.15 s. For the end-fire track (a), the experimental time was zero when the source was 1400 m (horizontal distance) from the last array element, and was 2750 s when the source was directly above hydrophone 30. Due to attenuation cross-correlations performed when the source was further from the array had significantly smaller amplitudes than those when the source was closer and hence this data has been normalised by the total energy for each correlation in order to see the evolution of the cross-correlation over the entire track. For both hyperbolae, the start and end of the experimental time correspond to distances approximately 1400 m from the array. The time at which the source passes the hyperbola apex occurs mid-experiment and can be seen in the graphs to be the time when the cross-correlation pattern is changing most dramatically (just under 3000 s for hyperbola-1 and approximately 2000 s for hyperbola-2). In both cases the correlation data collected before the source reached the apex is approximately symmetric to the data collected after the source passed this point. Actual differences result from imperfections in the source track, and changes in environment such as temporal changes in water column properties and differences in the environment due to range-dependence. In addition, the signals recorded would have been influenced by ship/source geometry; during the first half of each experiment the boat is between the source and the receivers, whilst during the second half it is not.

The end-fire unstacked cross-correlations look similar to the first half of the hyperbolae data. This is expected since the two methods are based upon the same principle. However, peaks in the correlation occur at a slightly earlier time for hyperbola-1 and at a

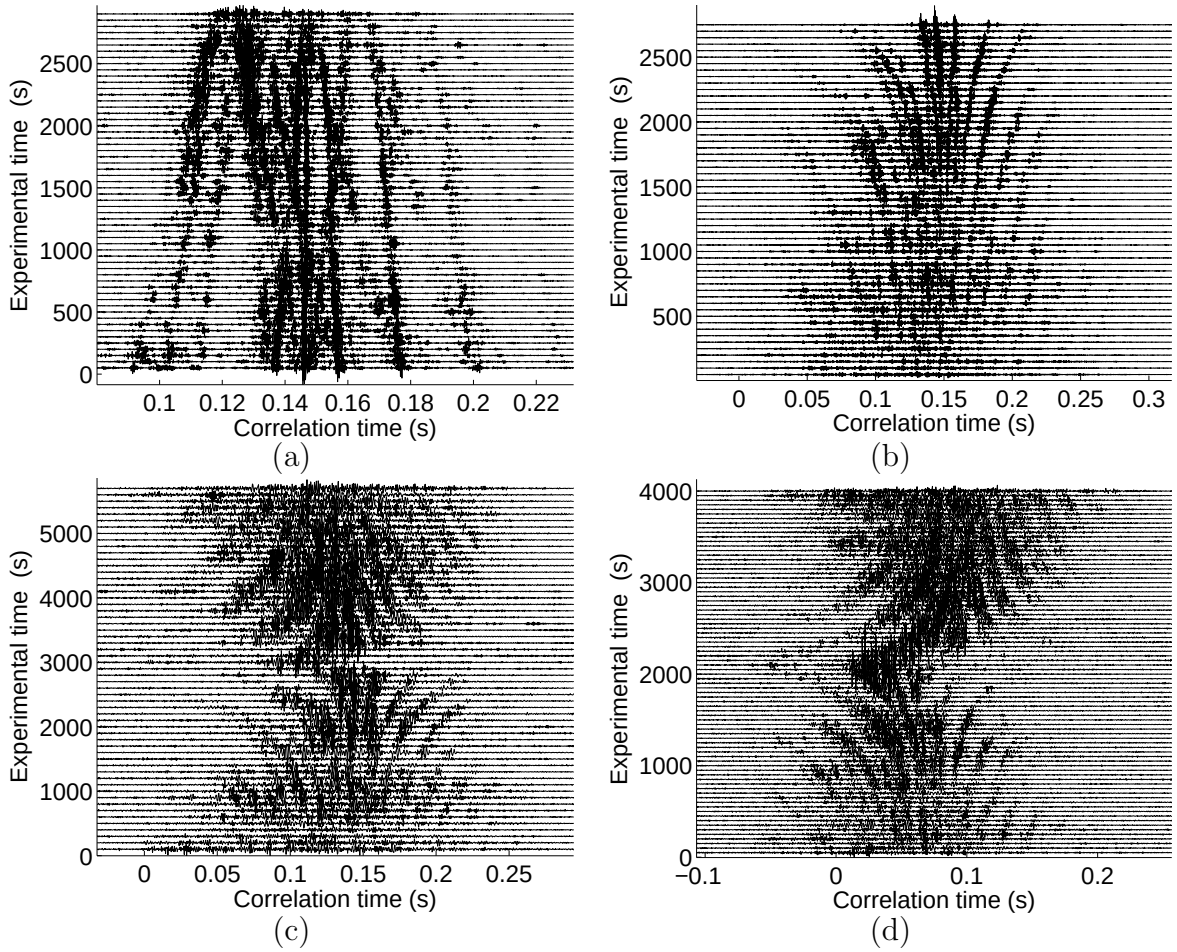

Figure 3. Unstacked cross-correlations of four runs plotted as a function of experimental time: (a) source lowering, (b) end-fire track, (c) hyperbola-1, and (d) hyperbola-2.

much earlier time for hyperbola-2. This is because the end-fire data should relate to the Green's function between hydrophones 30 and 5, whilst the data from hyperbolae-1 and -2 should relate to the Green's functions between hydrophones 28 and 5, and 16 and 5, respectively.

The existence of an apparent structure in each of the four data sets indicates that it is valid to attempt OAI with the data.

4. CONCLUSION

Ocean acoustic interferometry (OAI) refers to the process of recording the signals from a line of sources on two receivers and using this to infer the Green's function between the receivers. The time domain Green's function is approximated by summing, or integrating, over all source positions, the cross-correlations between the receivers.

Three source configurations were considered in this paper: source column, straight line towed source and hyperbolic towed source. Each of these configurations was briefly described and the mathematical relationship between the summed cross-correlations and the green's function between two receivers was given.

Experiments carried out during the SW06 sea trials which were designed to test each method of OAI were described in detail, and a preliminary graphical analysis of the data was presented. The preliminary analysis shows that there is an evolution of the cross-correlations as a function of range or depth. This is promising and hence a more

thorough analysis of the results has become ongoing work.

5. ACKNOWLEDGEMENTS

Work supported by Office of Naval Research under Grant No. N00014-05-1-0264. The first author is also appreciative of support from a Fulbright Postgraduate Award in Science and Engineering, sponsored by Clough Engineering, as well as support from the Defence Science and Technology Organisation, Australia.

REFERENCES

[1] O. I. Lobkis and R. L. Weaver, "On the emergence of the Green's function in the correlations of a diffuse field", *J. Acoust. Soc. Am.* **110**, 3011-3017 (2001).

[2] A. Derode, E. Larose, M. Tanter, J. de Rosny, A. Tourin, M. Campillo, and M. Fink, "Recovering the Green's function from field-field correlations in an open scattering medium", *J. Acoust. Soc. Am.* **113**, 2973-2976 (2003).

[3] K. Wapenaar, "Retrieving the elastodynamic Green's function of an arbitrary inhomogeneous medium by cross correlation", *Phys. Rev. Lett.* **93**, 254301 (2004).

[4] D-J. van Manen, J. O. A. Robertsson, and A. Curtis, "Modeling of wave propagation in inhomogeneous media", *Phys. Rev. Lett.* **94**, 164301 (2005).

[5] R. L. Weaver and O. I. Lobkis, "Ultrasonics without a source: Thermal fluctuation correlations at MHz frequencies", *Phys. Rev. Lett.* **87**, 134301 (2001).

[6] A. E. Malcolm, J. A. Scales, and B. A. van Tiggelen, "Extracting the Green function from diffuse, equipartitioned waves", *Phys. Rev. E* **70**, 015601 (2004).

[7] K. van Wijk, "On estimating the impulse response between receivers in a controlled ultrasonic experiment", *Geophysics* **71**, SI79-SI84 (2006).

[8] P. Roux, K. G. Sabra, W. A. Kuperman, and A. Roux, "Ambient noise cross correlation in free space: Theoretical approach", *J. Acoust. Soc. Am.* **117**, 79-84 (2005).

[9] P. Roux, W. A. Kuperman, and the NPAL Group, "Extracting coherent wave fronts from acoustic ambient noise in the ocean", *J. Acoust. Soc. Am.* **116**, 1995-2003 (2004).

[10] K. G. Sabra, P. Roux, and W. A. Kuperman, "Arrival-time structure of the time-averaged ambient noise cross-correlation function in an oceanic waveguide", *J. Acoust. Soc. Am.* **117**, 164-174 (2005).

[11] M. Siderius, C. H. Harrison, and M. B. Porter, "A passive fathometer technique for imaging seabed layering using ambient noise", *J. Acoust. Soc. Am.* **120**, 1315-1323 (2006).

[12] M. Campillo and A. Paul, "Long-range correlations in the diffuse seismic coda", *Science* **299**, 547-549 (2003).

[13] R. Snieder, "Extracting the Green's function from the correlation of coda waves: A derivation based on stationary phase", *Phys. Rev. E* **69**, 046610 (2004).

[14] N. M. Shapiro, M. Campillo, L. Stehly, and M. H. Ritzwoller, "High-resolution surface-wave tomography from ambient seismic noise", *Science* **307**, 1615-1618 (2005).

[15] P. Gerstoft, K. G. Sabra, P. Roux, W. A. Kuperman, and M. C. Fehler, "Green's functions extraction and surface-wave tomography from microseisms in southern California", *Geophysics* **71**, S123-S131 (2006).

[16] E. Larose, A. Khan, Y. Nakamura, and M. Campillo, "Lunar subsurface investigated from correlation of seismic noise", *Geophys. Res. Lett.* **32**, L16201 (2005).

[17] L. A. Brooks and P. Gerstoft, "Ocean acoustic interferometry", *J. Acoust. Soc. Am.*, accepted for publication **121**, (2007).

[18] A. Curtis, P. Gerstoft, H. Sato, R. Snieder, and K. Wapenaar, "Seismic interferometry - turning noise into signal", *The Leading Edge* **25**, 1082-1092 (2006).

[19] C. M. Bender and S. A. Orszag, *Advanced Mathematical Methods for Scientists and Engineers: Asymptotic Methods and Perturbation Theory*, McGraw-Hill, 1978.

[20] P. Roux and M. Fink, "Green's function estimation using secondary sources in a shallow water environment", *J. Acoust. Soc. Am.* **113**, 1406-1416 (2003).

[21] R. Snieder, K. Wapenaar, and K. Larner, "Spurious multiples in seismic interferometry of primaries", *Geophysics* **71**, SI111-SI124 (2006).

APPENDIX A: DERIVATION OF HYPERBOLIC SOURCE PATH

Consider Fig. 4, which is a geometrical view of the source p_n and receivers, A and B, from above.

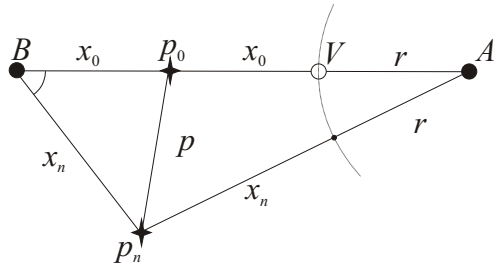

Figure 4. Geometrical construct for determining the equation governing the location of point p_n, which is a constant Δr further from A than B.

A virtual receiver V is located Δr from A along the line connecting A and B. The point p_n (p_0 along the line connecting A and B) is always Δr further from A than B:

$$p_n = (x_n \cos\phi, \pm x_n \sin\phi)\,. \tag{4}$$

From geometry:

$$(x_n + \Delta r)^2 = x_n^2 + (2x_o + \Delta r)^2 - 2(x_n)(2x_o + \Delta r)\cos(\phi). \tag{5}$$

Rearranging to express in terms of ϕ yields

$$\phi = \cos^{-1}\left(\frac{2x_o^2 + 2x_o\Delta r - x_n\Delta r}{x_n\,(2x_o + \Delta r)}\right). \tag{6}$$

The points p_n therefore form a hyperbola which has its asymptotic origin at the point midway between the two physical receivers A and B, its x-intercept at the midpoint of the B and the virtual receiver V, and its focus at the B. If the origin of the system is assumed to be at the first receiver and the second physical receiver lies along the positive x-axis, the governing equation can then be written in the form:

$$x^2 = -\sqrt{a^2\left(1 + \frac{y^2}{b^2}\right)} - c, \tag{7}$$

where $a = \frac{\Delta r}{2}$, $c = a - x_0$ (x_0 is the location where the hyperbola crosses the x-axis), and $b = -\sqrt{c^2 - a^2}$. The hyperbolic tow-source can be considered to be a similar geometrical set-up as the straight line scenario, although in this case, the horizontal distance in path length is a constant value of $x_A - x_V$. The resulting cross-correlation sum will therefore relate to the Green's function between the virtual receiver V and receiver A rather than the Green's function between the two physical receivers.